Influence of quantum confinement on the electronic structure of the transition metal sulfide TS_2

A. Kuc, N. Zibouche, and T. Heine
School of Engineering and Science, Jacobs University Bremen, Campus Ring 1, 28759 Bremen, Germany
(Received 22 February 2011; revised manuscript received 27 April 2011; published 30 June 2011)

Bulk MoS_2, a prototypical layered transition-metal dichalcogenide, is an indirect band gap semiconductor. Reducing its slab thickness to a monolayer, MoS_2 undergoes a transition to the direct band semiconductor. We support this experimental observation by first-principle calculations and show that quantum confinement in layered d-electron dichalcogenides results in tuning the electronic structure. We further studied the properties of related TS_2 nanolayers (T = W, Nb, Re) and show that the isotopological WS_2 exhibits similar electronic properties, while NbS_2 and ReS_2 remain metallic independent of the slab thickness.

DOI: 10.1103/PhysRevB.83.245213 PACS number(s): 71.20.Nr, 73.22.−f

I. INTRODUCTION

Layered transition-metal dichalcogenides (LTMDCs) of TX_2 type (T = Mo, W, Nb, Re, Ti, Ta, etc., X = S, Se, Te, etc.) have been studied extensively on the experimentally and theoretically for the last 40 years.[1–17] Molybdenum disulfide (MoS_2) is a prototypical LTMDC, which is composed of two-dimensional S–Mo–S sheets stacked on the top of one another, as shown in Fig. 1. Each sheet is trilayered with a Mo atom in the middle that is covalently bonded to six S atoms located in the top and bottom layers. The bonding between the adjacent S–Mo–S sheets is much weaker and they are held together by weak interlayer bonds leading to the quasi-2D character of MoS_2.

Due to the weak forces between the sheets and the anisotropic character of LTMDCs, shearing takes place more easily even under high pressure, leading to lubricant applications.[3,18] Other applications, such as catalysis, optoelectronics, and photovoltaics, have been proposed and investigated.[1,4,5,19–21] A single layer of MoS_2 was recently used to realize a field-effect transistor with HfO_2 as a gate insulator.[22] The transistor exhibits a room-temperature current on/off ratio exceeding 1×10^8 and mobility comparable to the mobility of thin silicon films or graphene nanoribbons. Two-dimensional sheets of layered materials can be produced nowadays by, e.g., liquid exfoliation, what was successfully performed in the case of transition-metal dichalcogenides by Coleman *et al.*[23]

The electronic structure of various bulk TMDCs and a monolayer of MoS_2 have been previously studied throughout *ab initio* calculations using the plane waves approach or local basis functions.[7,9,10,12,14] MoS_2 is an indirect band gap material in its bulk form, which recently was shown to become a direct band gap semiconductor when thinned to a monolayer.[12,16,24] Therefore, few-layer-MoS_2 materials can have their band gaps tuned and their values shift from the bulk value by at least 500 meV due to quantum size effects.

In this paper, we have studied slab-thickness-dependent electronic properties of TS_2 type, where T = Mo, W, Re, and Nb. The first-principle calculations were performed using localised Gaussian basis functions and compared to the available experimental data and plane wave calculations. The results show that the indirect-direct band gap transition also holds for WS_2. The band structures of ReS_2 and NbS_2 reveal metallic character and therefore, no such transition appears. It can be expected that the size-dependent phenomenon of band gap transition will occur also for other dichalcogenides, such as $MoSe_2$, WSe_2, $MoTe_2$, or WTe_2. This study is in progress and will be the subject of our next communication.

II. METHODS

In this work, we have studied LTMDCs of TS_2 type, where T = Mo, W, Re, and Nb. All structures have hexagonal symmetry and belong to the $P6_3/mmc$ space group. ReS_2 is a triclinic system but for the purposes of a direct comparison, we have used hexagonal symmetry. The monolayers and polylayers were cut out from the fully optimized bulk structures as (0 0 1) surfaces. Different numbers of layers were considered in this study: mono-, bi-, and quadrilayers, as well as, six- and eight-layered structures.

First-principle calculations were performed on the basis of density functional theory (DFT) as implemented in the CRYSTAL09 code.[25] The exchange and correlation terms were described using general gradient approximation (GGA) in the scheme of PBE (Perdew-Burke-Ernzerhof)[26] and PBE

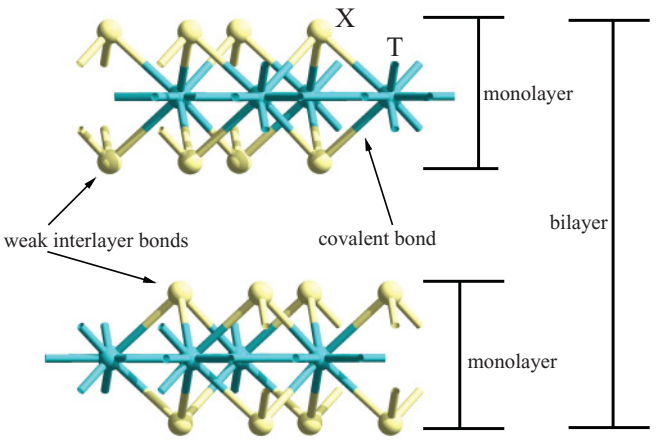

FIG. 1. (Color online) The atomic structure of layered transition-metal dichalcogenides of TX_2 type (T, transition metal; X, chalcogenide). Different sheets of TX_2 are composed of three atomic layers X–T–X, where T and X are covalently bonded. Sheets are held together by weak interlayer bonds.

TABLE I. Calculated and experimental lattice parameters of hexagonal transition-metal dichalcogenides in the form of TX_2 (T = Mo, W, Nb, Re; X = S, Se). Results obtained at the DFT/PBE level. In parentheses, data obtained at the DFT/PBE0 level are given.

	Theory		Expt. (Refs. 1, 2, 6)	
Structure	a	c	a	c
MoS_2	3.173 (3.143)	12.696 (12.583)	3.160	12.295
WS_2	3.164 (3.139)	12.473 (12.380)	3.154	12.362
NbS_2	3.332 (3.313)	12.106 (12.074)	3.310	11.890
ReS_2	3.300 (3.275)	12.724 (12.148)	...	...

hybrid (PBE0) functionals.[27] The following Gaussian basis sets were used: Mo_SC_HAYWSC-311(d31)G_cora_1997 (for Mo atoms), W_cora_1996 (for W atoms), Nb_SC_HAYWSC-31(d31)G_dallolio_1996 (for Nb atoms), Re_cora_1991 (for Re atoms), and S_86-311G*_lichanot_1993 (for S atoms). The chalcogenide atoms were calculated using full-electron basis sets, while for the heavy elements, the effective core potential (ECP) approach was employed. The large-core ECP has been chosen, what leaves only the valence electrons to be explicitly described on the metal sites: 4d and 5sp for Mo and Nb, 5d and 6sp for W and Re.

In CRYSTAL09 code, the 3D and 2D structures are treated as crystal and slab structures, respectively, therefore, in the case of layers there is no need to introduce vacuum.

Optimization of initial experimental structures was performed using analytical energy gradients with respect to atomic coordinates and unit cell parameters within a quasi-Newton scheme combined with the BFGS (Broyden-Fletcher-Goldfarb-Shanno) scheme for Hessian updation. The optimized lattice parameters for all the studied materials are given in Table I.

The shrinking factor (commensurate grid of k-points in reciprocal space at which the KS matrix is diagonalized) for bulk and layered structures was set to 8, what results in the corresponding number of 50 and 30 k-points in the irreducible Brillouin zone, respectively. The mesh of k-points was obtained according to the scheme proposed by Monkhorst and Pack.[28] Band structures were calculated along the high symmetry points using the path Γ–M–K–Γ.

III. RESULTS AND DISCUSSION

We have studied electronic properties of TS_2 layered structures with respect to the slab thickness of the systems. Bulk structures as well as mono- and polylayers were considered. DFT is widely used in the field of solid-state physics and it gives excellent structural parameters (see Table I) and charge distribution; however, typically it does not represent the electronic structure correctly. Therefore, we have introduced two different exchange-correlation functionals (PBE and PBE0) to address this problem specifically.

Figures 2 and 3 show band structures of MoS_2 and WS_2, respectively, calculated using PBE functional and going from bulk to a monolayer. (For band structures results using PBE0 functional see supplemental material).[29]

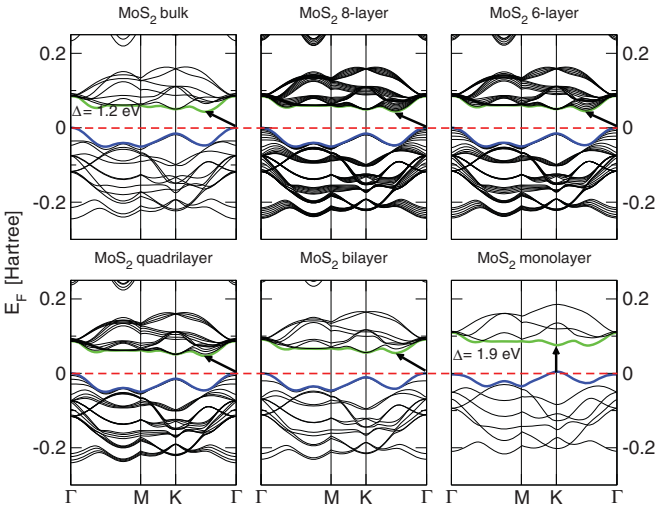

FIG. 2. (Color online) Band structures of bulk MoS_2, its monolayer, as well as, polylayers calculated at the DFT/PBE level. The horizontal dashed lines indicate the Fermi level. The arrows indicate the fundamental band gap (direct or indirect) for a given system. The top of valence band (blue/dark gray) and bottom of conduction band (green/light gray) are highlighted.

The results show that bulk MoS_2 and WS_2 are indirect-gap semiconductors. The fundamental band gap originates from transition from the top of valence band situated at Γ to the bottom of conduction band halfway between Γ and K high symmetry points. The optical direct band gap is situated at K point. As the number of layers decreases, the fundamental indirect band gap increases and becomes so high in the monolayer that the material changes into a 2D direct band gap semiconductor. At the same time, the optical direct gap (at the K point) stays almost unchanged (independent of the slab thickness) and close to the value of the optical direct band gap

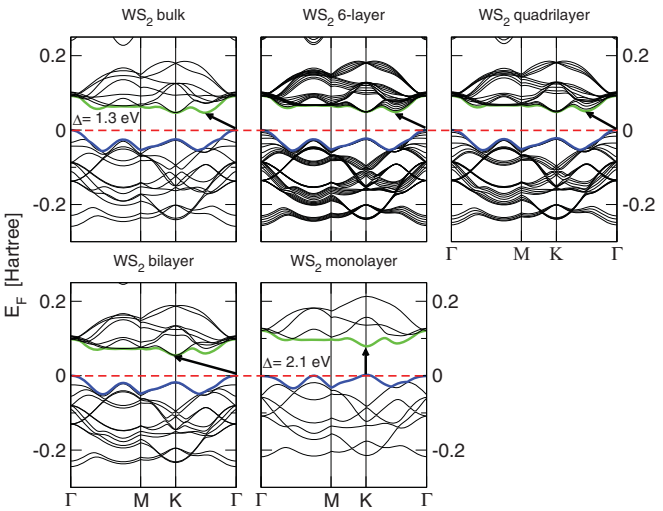

FIG. 3. (Color online) Band structures of bulk WS_2, its monolayer, as well as, polylayers calculated at the DFT/PBE level. The horizontal dashed lines indicate the Fermi level. The arrows indicate the fundamental band gap (direct or indirect) for a given system. The top of valence band (blue/dark gray) and bottom of conduction band (green/light gray) are highlighted.

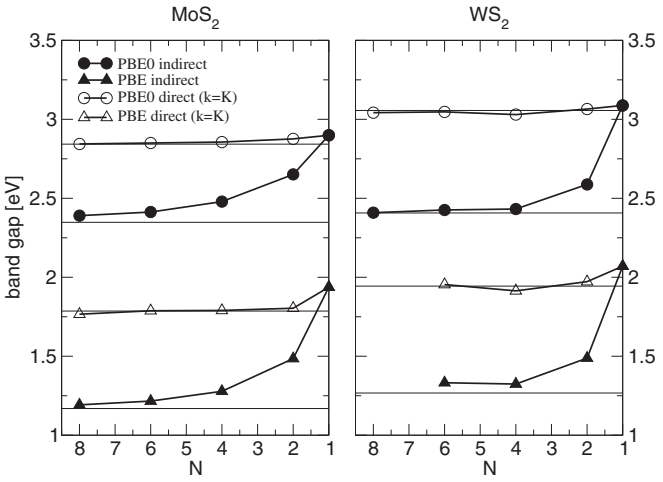

FIG. 4. Calculated direct and indirect band gap values of MoS_2 and WS_2 N-layer slabs. The horizontal solid lines indicate the band gaps of bulk structures.

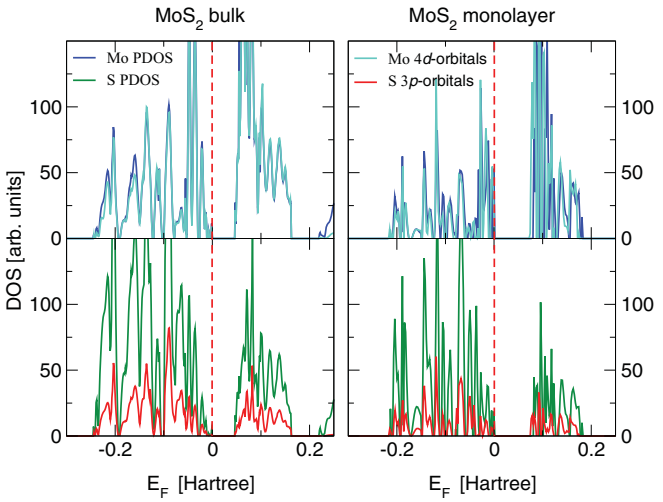

FIG. 5. (Color online) Partial density of states of bulk MoS_2 and its monolayer calculated as the DFT/PBE. The projections of Mo and S atoms are given together with the contributions from $4d$ and $3p$ orbitals of Mo and S, respectively. The vertical dashed lines indicate the Fermi level.

(at the K point) of a bulk system. These results are visualized better in Fig. 4 , where the band gap of MoS_2 and WS_2 are plotted against the number of layers.

There is a significant difference in the band gap values calculated using PBE and PBE0 functionals. Comparing the results with the available experimental data, one can see that the PBE functional performs better. The fundamental indirect band gap of bulk MoS_2 is 1.23 eV (Ref. 4) and our value of 1.2 eV agrees perfectly at the PBE level, while it is overestimated by around 1 eV using PBE0 hybrid functional. Similarly, the band gap of WS_2, with experimental value of 1.35 eV,[4] is 1.3 eV at the PBE level and 2.4 eV using PBE0. The experimental direct band gaps (at the K points) of MoS_2 and WS_2 are 1.74 and 1.79 eV, respectively.[4] Our DFT/PBE calculations give values of 1.8 and 1.9 eV for MoS_2 and WS_2, respectively. Again, the PBE0 results are overestimated by around 1 eV .

Li *et al.*,[14] using GGA/PBE functional and the plane wave approach, obtained band gap of 0.79 eV for the bulk MoS_2. For the same system, Matte *et al.*[16] have obtained 1.1 and 1.70 eV for the indirect and direct band gap, respectively, using GGA/PBE and DZP basis set. Using Perdew-Wang exchange-correlation functional and self-consistent pseudopotential, Arora *et al.*[11] have obtained the indirect band gap of 1.32 eV for the WS_2 bulk.

Decreasing the number of layers causes progressive shift in the indirect gap up to 1.9 and 2.1 eV for MoS_2 and WS_2, respectively. The change in the indirect gap energy is significantly larger than that of the direct gap (at the K point), which increased by around 0.1 eV. Similar results were found by Mak *et al.*[13] for MoS_2.

The band gaps of bulk structures are in the range of near infrared. Reducing the number of monolayers in the material to just a few layers causes the blueshift in absorption features and shifts the band gap to the range of the visible light. These materials can be, therefore, interesting in optoelectronics.

These unusual electronic structures of MoS_2 and WS_2, and the resulting optical properties come from the d-electron orbitals that dominate the valence and conduction bands (see Fig. 5 for MoS_2). The projected density of states (PDOS) of TS_2 shows that p-states of sulfur atoms hybridize with the d-states of the transition metal atoms at the top of valence band and the bottom of conduction band. The core states are dominated by the s-orbitals of the chalcogenide atom.

We have also studied the role of quantum confinement in niobium and rhenium disulfides and if their band gaps can be tuned by changing the slab thickness of the material. The electronic band structures of NbS_2 and ReS_2 (see Fig. 6) are different from those discussed above, especially close to the Fermi level. Although all the studied sulfides are isotopological, the NbS_2 and ReS_2 materials have metallic character independent of the number of layers.

The metallic character of NbS_2 comes from the fact that the $4d_{z^2}$ orbital is half-filled and results in a band that crosses the Fermi level in several points in the Brillouin zone. The band

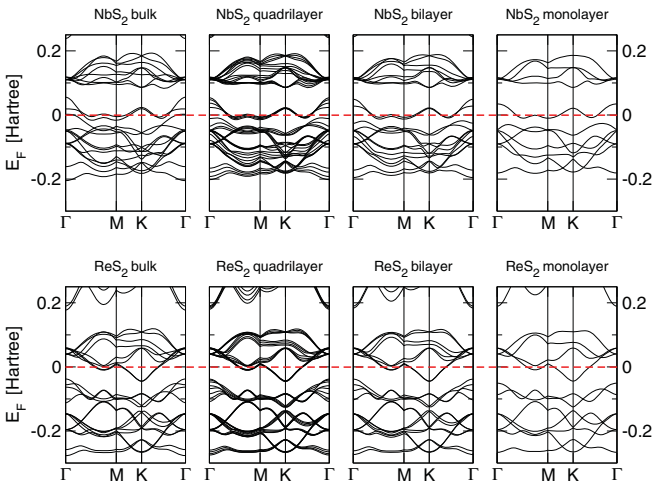

FIG. 6. (Color online) Band structures of bulk NbS_2 and ReS_2, their monolayer, as well as, polylayers calculated at the DFT/PBE level. The horizontal dashed lines indicate the Fermi level.

at the Fermi level is derived primarily from these 4*d*-orbitals and becomes separated from all other states in a monolayer.

The structure of ReS_2 studied here is of the same symmetry as all the other LTMDCs, even though the experimentally obtained material is triclinic. ReS_2 has one electron per metal atom more than MoS_2 and has a metallic character similar to NbS_2. The band that crosses the Fermi level comes from the 5*d*-orbitals of Re atoms. Unlike NbS_2, this band is not separated even in the monolayer and the electronic structure in the vicinity of the Fermi level is determined by short-range interactions in the sulfur 3*p* and rhenium 5*d* band complex.

For both, NbS_2 and ReS_2, the electronic structure of a bulk can be resemble by a single layer of these compounds.

IV. CONCLUSIONS

We have studied layered transition-metal dichalcogenides in form of TS_2 by means of GGA-DFT (PBE) and a hybrid functional (PBE0). The former was found to match experimental results for the band gap of the bulk phases within less than 0.1 eV, while PBE0 overestimates the band gap by 1 eV, but gives otherwise very similar band structures. Our DFT, at the PBE level, supports the recent findings of Splendiani *et al.*[12] for MoS_2: the material changes its electronic properties from an indirect semiconductor in the bulk phase to a direct semiconductor in the monolayer, an interesting phenomenon with potential application for optical devices. We show that WS_2 has very similar properties and can be considered as alternative material. On the other hand, both ReS_2 and NbS_2 systems have metallic character independent of the number of layers.

The LTMDCs, if mixed together, have interesting and promising technological potential, especially for nanoelectronics and catalysis. Therefore, we are presently working on the properties of doped structures of transition-metal dichalcogenides.

[1] J. A. Wilson and A. D. Yoffe, Adv. Phys. **18**, 193 (1969).
[2] L. F. Mattheis, Phys. Rev. B **8**, 3719 (1973).
[3] L. F. Mattheis, Phys. Rev. Lett. **30**, 784 (1973).
[4] K. K. Kam and B. A. Parkinson, J. Phys. Chem. **86**, 463 (1982).
[5] R. Coehoorn, C. Haas, and R. A. Degroot, Phys. Rev. B **35**, 6203 (1987).
[6] R. Coehoorn, C. Haas, J. Dijkstra, C. J. F. Flipse, R. A. Degroot, and A. Wold, Phys. Rev. B **35**, 6195 (1987).
[7] K. Kobayashi and J. Yamauchi, Phys. Rev. B **51**, 17085 (1995).
[8] J. P. Wilcoxon, P. P. Newcomer, and G. A. Samara, J. Appl. Phys. **81**, 7934 (1997).
[9] A. H. Reshak and S. Auluck, Phys. Rev. B **71**, 155114 (2005).
[10] S. Lebegue and O. Eriksson, Phys. Rev. B **79**, 115409 (2009).
[11] G. Arora, Y. Sharma, V. Sharma, G. Ahmed, S. K. Srivastava, and B. L. Ahuja, J. Alloys Compd. **470**, 452 (2009).
[12] A. Splendiani, L. Sun, Y. B. Zhang, T. S. Li, J. Kim, C. Y. Chim, G. Galli, and F. Wang, Nano Lett. **10**, 1271 (2010).
[13] K. F. Mak, C. Lee, J. Hone, J. Shan, and T. F. Heinz, Phys. Rev. Lett. **105**, (2010).
[14] W. Li, J. F. Chen, Q. Y. He, and T. Wang, Physica B **405**, 2498 (2010).
[15] N. L. Heda, A. Dashora, A. Marwal, Y. Sharma, S. K. Srivastava, G. Ahmed, R. Jain, and B. L. Ahuja, J. Phys. Chem. Solids **71**, 187 (2010).
[16] H. S. S. R. Matte, A. Gomathi, A. K. Manna, D. J. Late, R. Datta, S. K. Pati, and C. N. R. Rao, Angew. Chem., Int. Ed. **49**, 4059 (2010).
[17] B. Liu, Y. H. Han, C. X. Gao, Y. Z. Ma, G. Peng, B. J. Wu, C. L. Liu, Y. Wang, T. J. Hu, X. Y. Cui, W. B. Ren, Y. Li, N. N. Su, H. W. Liu, and G. T. Zou, J. Phys. Chem. C **114**, 14251 (2010).
[18] C. Drummond, N. Alcantar, J. Israelachvili, R. Tenne, and Y. Golan, Adv. Funct. Mater. **11**, 348 (2001).
[19] R. Tenne and A. Wold, Appl. Phys. Lett. **47**, 707 (1985).
[20] W. Sienicki and T. Hryniewicz, Solar Energy Mater. Sol. Cells **43**, 67 (1996).
[21] E. Gourmelon, O. Lignier, H. Hadouda, G. Couturier, J. C. Bernede, J. Tedd, J. Pouzet, and J. Salardenne, Solar Energy Mater. Sol. Cells **46**, 115 (1997).
[22] B. Radisavljevic, A. Radenovic, J. Brivio, V. Giacometti, and A. Kis, Nat. Nanotechnol. **6**, 147 (2011).
[23] J. N. Coleman, M. Lotya, A. O'Neill, S. D. Bergin, P. J. King, U. Khan, K. Young, A. Gaucher, S. De, R. J. Smith, I. V. Shvets, S. K. Arora, G. Stanton, H. Y. Kim, K. Lee, G. T. Kim, G. S. Duesberg, T. Hallam, J. J. Boland, J. J. Wang, J. F. Donegan, J. C. Grunlan, G. Moriarty, A. Shmeliov, R. J. Nicholls, J. M. Perkin, E. M. Grieveson, K. Theuwissen, D. W. McComb, P. D. Nellist, and V. Nicolosi, Science **331**, 568 (2011).
[24] T. S. Li and G. L. Galli, J. Phys. Chem. C **111**, 16192 (2007).
[25] R. Dovesi, V. R. Saunders, R. Roetti, R. Orlando, C. M. Zicovich-Wilson, F. Pascale, B. Civalleri, K. Doll, N. M. Harrison, I. J. Bush, P. D'Arco, and M. Llunell, *CRYSTAL09 User's Manual* (University of Torino, Torino, 2009).
[26] J. P. Perdew, K. Burke, and M. Ernzerhof, Phys. Rev. Lett. **77**, 3865 (1996).
[27] J. P. Perdew, M. Emzerhof, and K. Burke, J. Chem. Phys. **105**, 9982 (1996).
[28] H. J. Monkhorst and J. D. Pack, Phys. Rev. B **13**, 5188 (1976).
[29] See Supplemental Material at http://link.aps.org/supplemental/10.1103/PhysRevB.83.245213 for the electronic structures of TS_2 bulk, mono- and poly-layers calculated using PBE0 functional.